





Complete T_c suppression and Néel triplets mediated exchange in antiferromagnet-superconductor-antiferromagnet trilayers

Lina Johnsen Kamra ^{1,2,*},† Simran Chourasia ^{2,*} G. A. Bobkov,³ V. M. Gordeeva ³,
I. V. Bobkova,^{3,4} and Akashdeep Kamra ²

¹Center for Quantum Spintronics, Department of Physics, Norwegian University of Science and Technology, NO-7491 Trondheim, Norway

²Condensed Matter Physics Center (IFIMAC) and Departamento de Física Teórica de la Materia Condensada, Universidad Autónoma de Madrid, E-28049 Madrid, Spain

³Moscow Institute of Physics and Technology, Dolgoprudny, Moscow 141700, Russia

⁴National Research University Higher School of Economics, Moscow 101000, Russia



(Received 20 June 2023; revised 13 September 2023; accepted 9 October 2023; published 19 October 2023)

An antiferromagnetic insulator (AFMI) bearing a compensated interface to an adjacent conventional superconductor (S) has recently been predicted to generate Néel triplet Cooper pairs, whose amplitude alternates sign in space. Here, we theoretically demonstrate that such Néel triplets enable control of the superconducting critical temperature in an S layer via the angle between the Néel vectors of two enclosing AFMI layers. This angle dependence changes sign with the number of S monolayers providing a distinct signature of the Néel triplets. Furthermore, we show that the latter mediate a similarly distinct exchange interaction between the two AFMIs' Néel vectors.

DOI: [10.1103/PhysRevB.108.144506](https://doi.org/10.1103/PhysRevB.108.144506)

I. INTRODUCTION

Hybrids comprising a conventional spin-singlet superconductor (S) and one or more magnetic layers realize unconventional superconductivity and Cooper pairs, thereby enabling intriguing physics and potential applications [1–7]. The central role of magnets in this engineering of superconductivity is to induce a spin-splitting field which generates spin-triplet Cooper pairs from their spin-singlet counterparts available in S [8–10]. This also reduces the superconducting critical temperature T_c . A canonical structure sandwiches a thin S layer between two ferromagnet (FM) layers and enables control over the T_c via the relative angle α between the two FM magnetizations [11–19]. The dominant effect in this trilayer is the addition (cancellation) of spin-splitting fields from the two FMs when their magnetizations are parallel (antiparallel), resulting in the smallest (largest) T_c out of all FM configurations. This has been exploited to switch the S to its normal resistive state by controlling α via an applied magnetic field. This in turn admits a change of resistance from zero to a nonzero value, i.e., an infinite magnetoresistance [13,18,19].

The dipolar stray fields and GHz frequency magnons in FMs are parasitic detrimental influences in these devices. Employing antiferromagnets (AFMs) could significantly reduce these problems due to their zero net magnetization and higher magnon frequencies [20–23]. Furthermore, their two or more sublattices admit intriguing phenomena that bring along entirely novel functionalities [24]. However, early experiments with metallic AFMs found no influence on an adjacent S,

attributing this to their lack of net magnetization and thus spin-splitting field [25]. Subsequently, there have been theoretical predictions of spin-dependent transport at such AFM-S interfaces [26–29]. More recent experiments find a strong effect of the AFM on an adjacent S layer [30–35]. An AFM or antiferromagnetic insulator (AFMI) bearing an uncompensated interface to the adjacent S has recently been shown to induce spin splitting [23], which contributes to influencing the S.

Intriguingly and subsequently, even a compensated interface with an AFMI [Fig. 1(a)] was found to be spin active [36]. This has recently been understood as being due to the generation of the so-called Néel triplet Cooper pairs [37]. These have been so named as their amplitude changes sign from one lattice site to the next [Fig. 1(b)], while the magnitude varies slower on the coherence length scale. This alternation of sign is due to the Néel triplets being formed from interband pairing [37]. Alternately, within an extended Brillouin zone scheme, they can be considered to result from finite-momentum pairing. In contrast, the regular spin-triplet Cooper pairs generated by an adjacent FM only manifest a gradual spatial variation at the coherence length scale associated with the usual intraband pairing [2,3].

In this paper, we theoretically investigate how such Néel triplet Cooper pairs enable intriguing phenomena in an AFMI-S-AFMI trilayer [Fig. 1(a)]. Employing the Bogoliubov–de Gennes framework, we show that the critical temperature of the S layer depends on the angle θ between the two AFMIs' Néel vectors via a dominant $\cos\theta$ variation and a weaker $\sin^2\theta$ contribution. The dominant effect is due to the constructive [Fig. 1(c)] or destructive [Fig. 1(d)] interference between the Néel triplets generated by the two AFMI-S interfaces [37], while the $\sin^2\theta$ term is reminiscent of equal-spin triplets resulting from noncollinearity between

*These authors contributed equally to this work.

†lina.kamra@uam.es

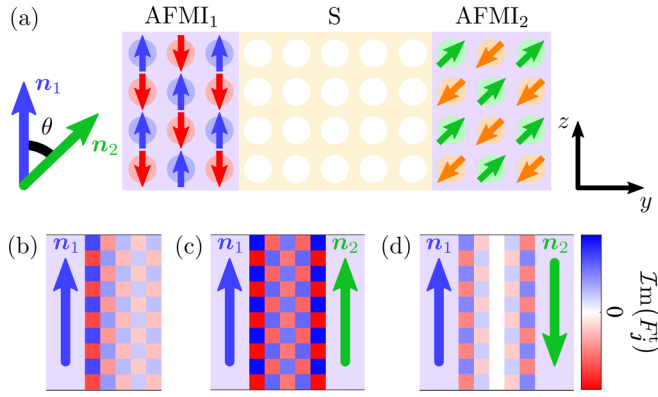


FIG. 1. Schematic depiction of the system and key underlying phenomena. (a) A conventional superconductor (S) is sandwiched between two compensated antiferromagnetic insulators (AFMIs) bearing Néel vectors \mathbf{n}_1 and \mathbf{n}_2 that subtend an angle θ . (b) In an AFMI-S bilayer, spatially alternating spin splitting induced by the AFMI predominantly generates Néel spin-triplet Cooper pairs characterized by a checkerboard pattern of their amplitude F_j^t [37], thus manifesting an alternating spatial parity. (c) In an AFMI-S-AFMI trilayer with odd number (considered 5 here) of S monolayers and $\theta = 0$, the Néel triplets generated by the two AFMIs interfere constructively. This results in more induced spin triplets and larger weakening of the spin-singlet superconductivity. (d) If instead $\theta = \pi$, the Néel triplets from the two AFMI-S interfaces interfere destructively and superconductivity is weakened less. This dependence of the superconducting state on θ is reversed when the number of S monolayers is even due to the checkerboard pattern associated with the Néel triplets.

the two Néel vectors [38–41]. For large enough AFMI-S interfacial exchange coupling, a complete and abrupt suppression of superconductivity (i.e., $T_c \rightarrow 0$) is achieved. Due to the alternating sign of Néel triplet correlations, the T_c vs θ dependence reverses when the number of S monolayers changes parity, providing a distinct and unique signature of the Néel triplets' role. By computing the superconducting free-energy density as a function of θ , we further demonstrate that the generated Néel Cooper pairs mediate coupling between the two AFMIs' Néel vectors exhibiting the signature parity effect with the S monolayers number. Our theoretical results suggest a direct experimental probe of these recently predicted Néel triplets [37] while enabling antiferromagnetic superconducting spintronics devices.

II. SYSTEM AND THEORETICAL MODEL

We consider a thin-film superconductor which on each side is interfacing an antiferromagnetic insulator, as schematically depicted in Fig. 1(a). While electron hopping is only allowed within the S layer, the two AFMIs impose a local spin splitting via interfacial exchange onto the atomic layer closest to the S-AFMI interfaces [23,37]. We can thus describe the system by the Hamiltonian

$$H = -t \sum_{(i,j),\sigma} c_{i,\sigma}^\dagger c_{j,\sigma} - \mu \sum_{j,\sigma} c_{j,\sigma}^\dagger c_{j,\sigma} - \frac{J}{2} \sum_j \mathbf{M}_j \cdot \mathbf{S}_j + \sum_j \left(\frac{|\Delta_j|^2}{U} + \Delta_j^* c_{j,\downarrow} c_{j,\uparrow} + \Delta_j c_{j,\uparrow}^\dagger c_{j,\downarrow}^\dagger \right). \quad (1)$$

Here, $c_{j,\sigma}^{(\dagger)}$ is the annihilation (creation) operator associated with an electron of spin σ at lattice site $\mathbf{j} \equiv (j_z, j_y)$, t parametrizes electron hopping between nearest-neighbor sites within the S, $\mathbf{S}_j \equiv \sum_{\sigma,\sigma'} c_{j,\sigma}^\dagger \boldsymbol{\sigma}_{\sigma,\sigma'} c_{j,\sigma'}$ is the spin operator for S electrons with $\boldsymbol{\sigma}$ as the vector of Pauli matrices, and $\Delta_j \equiv -U \langle c_{j,\downarrow} c_{j,\uparrow} \rangle$ is the self-consistently evaluated mean-field superconducting gap [42]. The chemical potential μ is adjusted to fix the filling fraction, which we assume to be $n = 0.5$ here. We consider the S lattice to bear the size $N_z \times N_y$ with periodic boundary conditions along z [Fig. 1(a)]. As we consider ideal insulating antiferromagnets, their thicknesses do not influence the phenomena investigated here.

A local spin-splitting field $J\mathbf{M}_j/2$ is imposed by the two AFMIs onto the S interfacial monolayers ($j_z, 1$) and (j_z, N_y). Here, J parametrizes the AFMI-S interfacial exchange coupling. As depicted in Fig. 1(a), the magnetic moments in the first AFMI have a fixed orientation corresponding to the Néel vector $\mathbf{n}_1 = \mathbf{z}$ so that $\mathbf{M}_{(j_z,1)} = (-1)^{j_z-1} \mathbf{n}_1$. The Néel vector $\mathbf{n}_2 = [\cos(\theta)\mathbf{z} + \sin(\theta)\mathbf{y}]$ of the second AFMI leads to rotation of the local spin splitting oriented along $\mathbf{M}_{(j_z,N_y)} = (-1)^{j_z-1} \mathbf{n}_2$.

We numerically diagonalize the Hamiltonian in Eq. (1) by solving the Bogoliubov–de Gennes equation [42] self-consistently,

$$H = H_0 + \sum_n' E_n \gamma_n^\dagger \gamma_n, \quad (2)$$

with

$$H_0 = -N\mu - \sum_j \frac{|\Delta_j|^2}{U} - \frac{1}{2} \sum_n' E_n, \quad (3)$$

where \sum_n' denotes the sum over positive eigenenergies $E_n > 0$ only, $\{\gamma_n^\dagger\}$ is a set of unique fermion operators, and $N = N_z N_y$ is the total number of S lattice sites. The resulting solution provides complete information on the superconducting or normal state of the S layer.

III. CRITICAL TEMPERATURE CONTROL VIA θ

In order to examine the magnetoresistance and S layer's critical temperature dependence on the AFMIs, we numerically compute the superconducting critical temperature T_c . It is determined using a binary search algorithm locating the temperature at which the superconducting gap starts to increase from a near-zero initial guess upon its self-consistent evaluation [43,44].

To succinctly capture and present the T_c variation with θ for different thicknesses N_y of the S layer, we first parametrize T_c vs θ on symmetry grounds. This parametrization is only valid for small changes in T_c . For a small J , T_c is only weakly altered by the adjacent AFMIs and is expected to bear the dependence,

$$\tilde{T}_c(\theta) \equiv \frac{T_c(\theta)}{T_{c,0}} \equiv \Delta \tilde{T}_{c,\parallel} \cos \theta + \Delta \tilde{T}_{c,\perp} \sin^2 \theta + \tilde{T}_{c,\parallel}, \quad (4)$$

where $T_{c,0}$ is the critical temperature of the same S layer when it is not coupled to the AFMIs, i.e., assuming $J = 0$ in Eq. (1).

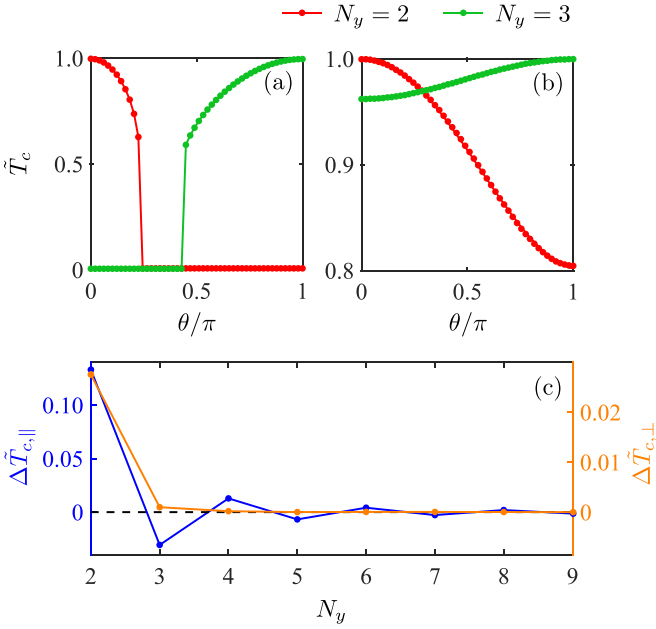


FIG. 2. Normalized critical temperature \tilde{T}_c variation with θ for (a) stronger and (b) weaker interfacial exchange coupling J . The variation is reversed when the number of S monolayers N_y changes from even to odd. A complete suppression of T_c is observed for the stronger J case (a), while the weaker exchange (b) results in a variation of T_c as per Eq. (4). (c) By fitting the numerically evaluated $\tilde{T}_c(\theta)$ to Eq. (4) for different thicknesses N_y , $\Delta\tilde{T}_{c,\parallel}$ and $\Delta\tilde{T}_{c,\perp}$ are obtained and studied for their thickness N_y dependence. The parity effect of $\Delta\tilde{T}_{c,\parallel}$ with respect to N_y results from the alternating sign of Néel triplets' amplitude, as discussed in Fig. 1. In all panels, $N_z = 202$. In (a), $U/t = 1$ and $J/t = 0.08$. In (b), $U/t = 1$ and $J/t = 0.02$. In (c), $U/t = 1.3$ and $J/t = 0.08$.

From Eq. (4) above, we see that

$$\begin{aligned}\Delta\tilde{T}_{c,\parallel} &= [\tilde{T}_c(0) - \tilde{T}_c(\pi)]/2, & \tilde{T}_{c,\parallel} &= [\tilde{T}_c(0) + \tilde{T}_c(\pi)]/2, \\ \Delta\tilde{T}_{c,\perp} &= \tilde{T}_c(\pi/2) - \tilde{T}_{c,\parallel}.\end{aligned}\quad (5)$$

In Eq. (4), the $\Delta\tilde{T}_{c,\parallel} \cos \theta$ term is expected due to the interference of zero-spin Néel triplets generated by the two AFMI-S interfaces [37], as briefly outlined in Fig. 1. It is analogous to the $\cos \theta$ dependence in FM-S-FM trilayers [11,12] and bears the symmetry of vectorial addition of the spin-splitting fields from the two AFMIs. The $\Delta\tilde{T}_{c,\perp} \sin^2 \theta$ term is expected from the generation of equal-spin triplets via the noncollinearity between \mathbf{n}_1 and \mathbf{n}_2 [38–41] as it is finite only when the two magnetic orders are noncollinear. In Eq. (4), $\Delta\tilde{T}_{c,\parallel}$ characterizes the T_c difference between parallel and antiparallel configurations. When it is positive (negative), the T_c is larger for the parallel (antiparallel) configuration of the magnetic orders. On the other hand, $\Delta\tilde{T}_{c,\perp}$ represents the change in T_c when going from parallel to perpendicular configurations. Together, $\Delta\tilde{T}_{c,\parallel}$ and $\Delta\tilde{T}_{c,\perp}$ provide a succinct parametrization to study and present T_c vs θ in our system. We emphasize that our numerical evaluation of T_c does not depend on or assume this parametrization [Eq. (4)].

In Fig. 2(a), we depict the \tilde{T}_c variation when the interfacial exchange is strong and results in a complete T_c suppression for certain θ . When the number of S monolayers $N_y = 2$, the

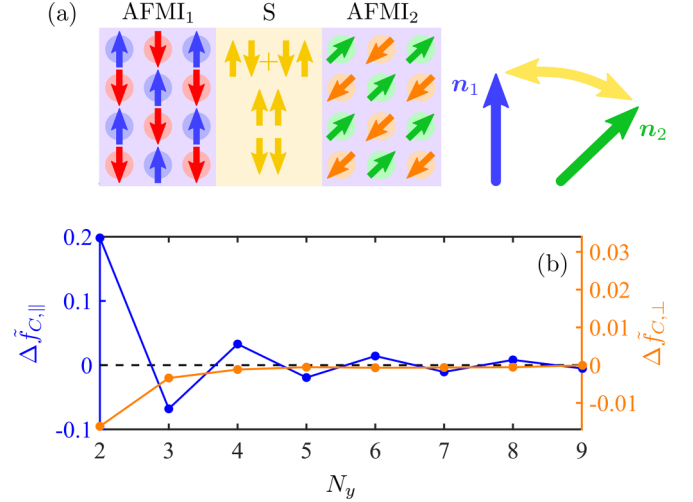


FIG. 3. (a) Spin-triplet Cooper pairs generated by the AFMIs mediate coupling between the two Néel vectors \mathbf{n}_1 and \mathbf{n}_2 . This coupling is captured by the superconducting condensate's contribution f_c to the θ dependence of the free energy density. (b) Fitting numerically evaluated f_c to Eq. (7) yields $\Delta\tilde{f}_{c,\parallel}$ and $\Delta\tilde{f}_{c,\perp}$, which are plotted vs N_y , thereby delineating the thickness dependence of the mediated coupling. We have employed $N_z = 202$, $U/t = 1.3$, $J/t = 0.05$, and $\beta t = 10^4$.

Néel triplets generated by the two AFMI-S interfaces interfere destructively for $\theta = 0$. This results in a weakening of the effect due to the AFMIs and a larger T_c at $\theta = 0$. For $N_y = 3$, the interference becomes constructive for $\theta = 0$ [Fig. 1(c)] due to the checkerboard pattern of the Néel triplets [Fig. 1(b)] and the T_c vs θ trend is reversed. When the exchange coupling J is small enough to avoid a complete suppression of T_c , the numerically evaluated $\tilde{T}_c(\theta)$ [Fig. 2(b)] is found to perfectly fit Eq. (4). The reversal of trends between $N_y = 2$ and 3 remains as before and is attributed to the interference and checkerboard effects.

Considering a filling fraction $n = 0.6$, we found a negligible dependence of T_c on θ . This is consistent with a much weaker generation of Néel triplets away from $n = 0.5$ corresponding to $\mu = 0$ [41]. Furthermore, for a direct comparison, we discuss plots analogous to Figs. 2(a) and 2(b) for a trilayer comprising a ferromagnetic insulator (FMI) instead of an AFMI in the Appendix. The FMI-S-FMI trilayer is found to exhibit a weaker T_c dependence, lack of an abrupt jump to 0 seen in Fig. 2(a), and no reversal of T_c variation between $N_y = 2$ and 3. This emphasizes the several unique features of our investigated AFMI-S-AFMI system. Here, we have considered AFMIs with zero net magnetic moments. In the presence of a finite magnetic moment due to canting [41], we expect the T_c variation to bear a small contribution reminiscent of the FMI-S-FMI case investigated in the Appendix.

Finally, Fig. 3(c) shows the dependence of $\Delta\tilde{T}_{c,\parallel}$ and $\Delta\tilde{T}_{c,\perp}$ on N_y obtained by fitting the numerically evaluated data to Eq. (4). $\Delta\tilde{T}_{c,\parallel}$, found to be an order of magnitude larger than $\Delta\tilde{T}_{c,\perp}$, exhibits a parity effect with N_y due to the checkerboard pattern of Néel triplets [Fig. 1(b)] and the resulting interference effects [Figs. 1(c) and 1(d)]. This further validates the argument presented above that the $\Delta\tilde{T}_{c,\parallel} \cos \theta$ term stems

from the Néel zero-spin triplets [37,41]. As $\Delta\tilde{T}_{c,\perp}$ stems from the regular equal-spin triplets generated by the noncollinearity between \mathbf{n}_1 and \mathbf{n}_2 [38–40], it exhibits a simple decay with N_y without any alternation of its sign.

The results presented above (Fig. 2) show that an infinite magnetoresistance [18], resulting from a switching between the normal resistive and superconducting states using an applied magnetic field, is achievable in the considered AFMI-S-AFMI trilayer by reorienting the Néel vector of one AFMI with respect to the other. Recent experiments already demonstrate manipulation of the Néel vector in an easy-plane AFMI, such as hematite above the Morin transition [45], using small magnetic fields [46]. Furthermore, a complete suppression of T_c [Fig. 1(a)] enables such a device at arbitrarily low temperatures. An observation of the parity effect with N_y [Fig. 2(c)] will additionally provide evidence in favor of these recently predicted Néel triplets.

IV. NÉEL TRIPLETS MEDIATED COUPLING BETWEEN THE ANTIFERROMAGNETIC INSULATORS

We have learned above how the generation of Néel triplets by the two AFMIs enables control over the superconducting state in an AFMI-S-AFMI trilayer. Now, we seek to examine the inverse effect, i.e., how the superconducting condensate enables a coupling between the two Néel vectors \mathbf{n}_1 and \mathbf{n}_2 [Fig. 3(a)]. This is distinct from the conventional exchange coupling between two magnetizations [11]. Since the latter vanishes in a typical AFMI, coupling two AFMIs is more challenging and rewarding. Furthermore, in an FMI-S-FMI trilayer, the coupling between the two magnetic orders mediated by Cooper pairs competes with a direct dipolar interaction between them. A lack of the latter in our AFMI-S-AFMI system makes the role of Cooper pairs more important.

To examine the desired coupling, we need to compute the S layer free-energy density f as a function of θ . It is given by $f = -(1/\beta N)\ln(Z)$, where the partition function Z is $Z = \text{Tr}[\exp(-\beta H)]$. Here, $\beta = 1/k_B T$ with k_B the Boltzmann constant and T the temperature. Inserting the diagonalized Hamiltonian Eq. (2) into the free-energy density expression above, we obtain

$$f = \frac{H_0}{N} - \frac{1}{\beta N} \sum_n^l \ln(1 + e^{-\beta E_n}), \quad (6)$$

which is evaluated numerically [36]. This free-energy density [Eq. (6)] includes the contribution of quasiparticles, which can also mediate a coupling between the two AFMIs [21,47–49]. Since we are interested in the superconducting condensate's role in mediating this coupling, we focus on the superconducting condensation energy density contribution $f_C \equiv f_N - f_S$ attributed to the Cooper pairs [50]. Here, f_N (f_S) denotes the free-energy density in the normal (superconducting) state and is obtained when $U = 0$ ($U \neq 0$) in the Hamiltonian Eq. (1).

Making symmetry-based and physical arguments similar to the ones put forward in assuming the T_c dependence Eq. (4),

we expect the relation

$$\begin{aligned} \tilde{f}_C(\theta) \equiv \frac{f_C(\theta)}{f_{C,0}} &\equiv \Delta\tilde{f}_{C,\parallel}(\mathbf{n}_1 \cdot \mathbf{n}_2) \\ &+ \Delta\tilde{f}_{C,\perp}(\mathbf{n}_1 \times \mathbf{n}_2)^2 + \tilde{f}_{C,\parallel}, \end{aligned} \quad (7)$$

where $f_{C,0}$ is the condensation energy for the same S layer without the adjacent AFMIs, i.e., considering $J = 0$ in Eq. (1). Furthermore, we have expressed θ in terms of the Néel unit vectors to emphasize and clarify their mutual coupling [Fig. 3(a)].

Evaluating $\tilde{f}_C(\theta)$ numerically, we find the results to fit Eq. (7) perfectly, thereby vindicating it and providing the desired $\Delta\tilde{f}_{C,\parallel}$ and $\Delta\tilde{f}_{C,\perp}$. These have been plotted in Fig. 3(b) for different number N_y of S monolayers. $\Delta\tilde{f}_{C,\parallel}$ originates from the Néel zero-spin triplets [37,41] and captures an exchange-like interaction between the two AFMIs' Néel orders. Consequently, it also bears the parity effect resulting from the alternating nature of the pairing amplitude [Fig. 1(b)]. On the other hand, $\Delta\tilde{f}_{C,\perp}$ represents an unconventional interaction originating from the equal-spin triplets induced by the noncollinearity between \mathbf{n}_1 and \mathbf{n}_2 .

Altogether, Fig. 3 delineates the thickness dependence of the desired coupling between the two AFMIs' Néel orders, which may find applications in control over AFMIs. At the same time, the similarity between Figs. 2(c) and 3(b) indicates the complementarity between and a common origin of the effects investigated here providing valuable insights into the Néel proximity effect and Cooper pairs.

V. CONCLUSION

Employing the Bogoliubov–de Gennes framework and numerical diagonalization of the Hamiltonian, we have demonstrated a control of the superconducting critical temperature (T_c) and a condensate-mediated coupling between the two Néel vectors in an AFMI-S-AFMI trilayer with compensated interfaces. Our investigated trilayer manifests various advantages over its conventional FMI-S-FMI counterpart including a stronger effect on T_c and no interference from magnetostatic fields in the coupling between the two magnetic orders. The demonstrated dependence of T_c on the two Néel vectors enables an infinite magnetoresistance in the current-in-plane geometry via switching between the normal and superconducting states of the S layer [18]. An interference between the spin-triplet Cooper pairs generated by the AFMI-S interfaces is further shown to enable coupling between the two AFMIs' Néel vectors \mathbf{n}_1 and \mathbf{n}_2 . The predominant coupling mediated by the Néel zero-spin triplets is exchange-like $\sim \mathbf{n}_1 \cdot \mathbf{n}_2$, while a weaker coupling of the form $\sim (\mathbf{n}_1 \times \mathbf{n}_2)^2$ is caused by equal-spin triplets. These phenomena are enabled by the recently predicted Néel triplet Cooper pairs [37] generated at such compensated AFMI-S interfaces. As a result they bear a distinct parity effect carrying signatures of the Néel triplets' alternating amplitude and should provide the means to experimentally observe them. Thus, our work paves the way for investigating a broad range of superconducting hybrids incorporating antiferromagnets including the effects of spin-orbit coupling. At the same time, the phenomena discussed here outline possibilities for exploiting the

broad range of advantages offered by antiferromagnets in superconducting spintronic devices and phenomena.

ACKNOWLEDGMENTS

S.C. and A.K. acknowledge financial support from the Spanish Ministry for Science and Innovation – AEI Grant No. CEX2018-000805-M (through the “Maria de Maeztu” Programme for Units of Excellence in R&D) and Grant No. RYC2021-031063-I funded by MCIN/AEI/10.13039/501100011033 and “European Union Next Generation EU/PRTR.” L.J.K. acknowledges financial support from the Research Council of Norway through its Centers of Excellence funding scheme, Project No. 262633, “QuSpin.” I.V.B., G.A.B., and V.M.G. acknowledge support from MIPT, Project No. FSMG-2023-0014.

APPENDIX: FERROMAGNET-SUPERCONDUCTOR-FERROMAGNET TRILAYER

Here, we consider trilayers comprised by ferromagnetic insulator (FMI) layers [see Fig. 4(a)] instead of the compensated antiferromagnetic insulator (AFMI) layers considered in the main text. Employing the same numerical routines, we evaluate T_c as a function of the angle θ between magnetic orders of the two FMI layers. The plots in Figs. 4(b) and 4(c) show data analogous to that in Figs. 2(a) and 2(b) of the main text, including use of the same parameter values.

There are two minor differences in the numerical method though. First, we needed to employ a larger value of N_z to adequately capture the superconducting properties. This is because the density of states for the AFMI-S-AFMI is larger than its FMI-S-FMI counterpart for the considered parameters. Thus, a larger number of lattice sites was needed to obtain convergent values for the FMI-S-FMI trilayer. Second, the algorithm for T_c evaluation needs to be modified and in each binary search iteration, the superconducting gap needs to be established self-consistently. This is because the FMI-S-FMI system manifests a first-order phase transition with temperature [9,10] for larger values of J . There are thus multiple stable solutions for the superconducting state for a range of parameters. Our updated T_c search algorithm overcomes all these complications. As a result, the numerical evaluation for the

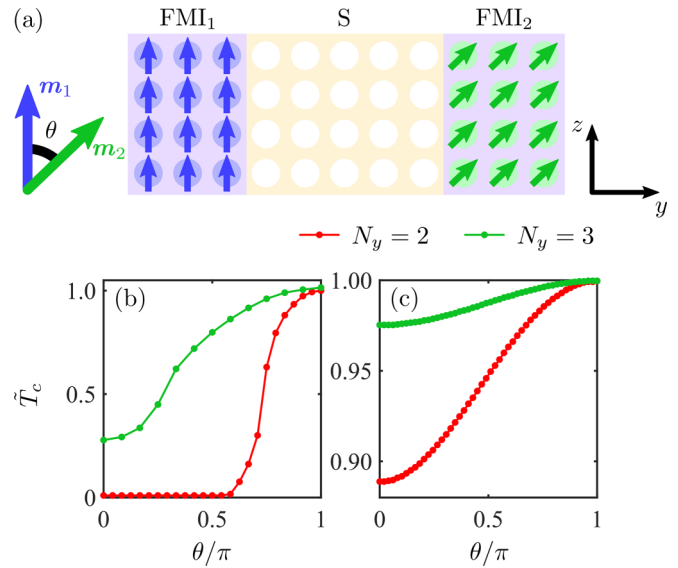


FIG. 4. (a) Schematic depiction of a system where the compensated AFMIs are replaced with ferromagnetic insulators (FMIs) with magnetization along m_1 and m_2 that subtend an angle θ . The normalized critical temperature \tilde{T}_c variation with θ is plotted for (b) stronger and (c) weaker interfacial exchange coupling J . Contrary to the AFMI/S/AFMI system, the variation is no longer reversed when the number of S monolayers N_y changes from even to odd. The weaker exchange (b) results in variation of T_c as per Eq. (4) in the main text. In both panels, $N_z = 402$ and $U/t = 1$. In (b), $J/t = 0.08$. In (c), $J/t = 0.02$.

FMI-S-FMI system was much more computationally intensive, resulting in our providing fewer data points in Fig. 4(b).

The numerically evaluated data plotted in Figs. 4(b) and 4(c) show that the variation of T_c is weaker in the case of FMI-S-FMI, as compared to the situation in AFMI-S-AFMI. Furthermore, the maximum T_c is always obtained at $\theta = \pi$, as expected [11]. There is no parity effect with the number of S layers, reinforcing our argument that the observed parity effect in AFMI-S-AFMI system is a smoking gun signature of the Néel triplets. Finally, Fig. 4(b) shows that for the FMI-S-FMI system, T_c varies smoothly with θ and there is no abrupt jump to 0, as what is seen for the AFMI-S-AFMI case.

- [1] M. Sigrist and K. Ueda, Phenomenological theory of unconventional superconductivity, *Rev. Mod. Phys.* **63**, 239 (1991).
- [2] A. I. Buzdin, Proximity effects in superconductor-ferromagnet heterostructures, *Rev. Mod. Phys.* **77**, 935 (2005).
- [3] F. S. Bergeret, A. F. Volkov, and K. B. Efetov, Odd triplet superconductivity and related phenomena in superconductor-ferromagnet structures, *Rev. Mod. Phys.* **77**, 1321 (2005).
- [4] Y. Tanaka, M. Sato, and N. Nagaosa, Symmetry and topology in superconductors—Odd-frequency pairing and edge states, *J. Phys. Soc. Jpn.* **81**, 011013 (2012).
- [5] M. Eschrig, Spin-polarized supercurrents for spintronics: A review of current progress, *Rep. Prog. Phys.* **78**, 104501 (2015).
- [6] J. Linder and J. W. A. Robinson, Superconducting spintronics, *Nat. Phys.* **11**, 307 (2015).
- [7] F. S. Bergeret, M. Silaev, P. Virtanen, and T. T. Heikkilä, Colloquium: Nonequilibrium effects in superconductors with a spin-splitting field, *Rev. Mod. Phys.* **90**, 041001 (2018).
- [8] K. Maki and T. Tsuneto, Pauli paramagnetism and superconducting state, *Prog. Theor. Phys.* **31**, 945 (1964).
- [9] A. M. Clogston, Upper limit for the critical field in hard superconductors, *Phys. Rev. Lett.* **9**, 266 (1962).
- [10] B. S. Chandrasekhar, A note on the maximum critical field of high-field superconductors, *Appl. Phys. Lett.* **1**, 7 (1962).
- [11] P. De Gennes, Coupling between ferromagnets through a superconducting layer, *Phys. Lett.* **23**, 10 (1966).

- [12] G. Deutscher and F. Meunier, Coupling between ferromagnetic layers through a superconductor, *Phys. Rev. Lett.* **22**, 395 (1969).
- [13] L. R. Tagirov, Low-field superconducting spin switch based on a superconductor/ferromagnet multilayer, *Phys. Rev. Lett.* **83**, 2058 (1999).
- [14] M. L. Kulić and M. Endres, Ferromagnetic-semiconductor-singlet-(or triplet) superconductor-ferromagnetic-semiconductor systems as possible logic circuits and switches, *Phys. Rev. B* **62**, 11846 (2000).
- [15] J. Y. Gu, C.-Y. You, J. S. Jiang, J. Pearson, Y. B. Bazaliy, and S. D. Bader, Magnetization-orientation dependence of the superconducting transition temperature in the ferromagnet-superconductor-ferromagnet system: CuNi/Nb/CuNi, *Phys. Rev. Lett.* **89**, 267001 (2002).
- [16] K. Westerholt, D. Sprungmann, H. Zabel, R. Brucas, B. Hjörvarsson, D. A. Tikhonov, and I. A. Garifullin, Superconducting spin valve effect of a V layer coupled to an antiferromagnetic [Fe/V] superlattice, *Phys. Rev. Lett.* **95**, 097003 (2005).
- [17] I. C. Moraru, W. P. Pratt, and N. O. Birge, Magnetization-dependent T_c shift in ferromagnet/superconductor/ferromagnet trilayers with a strong ferromagnet, *Phys. Rev. Lett.* **96**, 037004 (2006).
- [18] B. Li, N. Roschewsky, B. A. Assaf, M. Eich, M. Epstein-Martin, D. Heiman, M. Münzenberg, and J. S. Moodera, Superconducting spin switch with infinite magnetoresistance induced by an internal exchange field, *Phys. Rev. Lett.* **110**, 097001 (2013).
- [19] Y. Gu, G. B. Halász, J. W. A. Robinson, and M. G. Blamire, Large superconducting spin valve effect and ultrasmall exchange splitting in epitaxial rare-earth-niobium trilayers, *Phys. Rev. Lett.* **115**, 067201 (2015).
- [20] E. V. Gomonay and V. M. Loktev, Spintronics of antiferromagnetic systems (review article), *Low Temp. Phys.* **40**, 17 (2014).
- [21] V. Baltz, A. Manchon, M. Tsoi, T. Moriyama, T. Ono, and Y. Tserkovnyak, Antiferromagnetic spintronics, *Rev. Mod. Phys.* **90**, 015005 (2018).
- [22] T. Jungwirth, X. Marti, P. Wadley, and J. Wunderlich, Antiferromagnetic spintronics, *Nat. Nanotechnol.* **11**, 231 (2016).
- [23] A. Kamra, A. Rezaei, and W. Belzig, Spin splitting induced in a superconductor by an antiferromagnetic insulator, *Phys. Rev. Lett.* **121**, 247702 (2018).
- [24] L. Šmejkal, Y. Mokrousov, B. Yan, and A. H. MacDonald, Topological antiferromagnetic spintronics, *Nat. Phys.* **14**, 242 (2018).
- [25] J. J. Hauser, H. C. Theuerer, and N. R. Werthamer, Proximity effects between superconducting and magnetic films, *Phys. Rev.* **142**, 118 (1966).
- [26] I. V. Bobkova, P. J. Hirschfeld, and Y. S. Barash, Spin-dependent quasiparticle reflection and bound states at interfaces with itinerant antiferromagnets, *Phys. Rev. Lett.* **94**, 037005 (2005).
- [27] B. M. Andersen, I. V. Bobkova, P. J. Hirschfeld, and Y. S. Barash, Bound states at the interface between antiferromagnets and superconductors, *Phys. Rev. B* **72**, 184510 (2005).
- [28] B. M. Andersen, I. V. Bobkova, P. J. Hirschfeld, and Y. S. Barash, $0-\pi$ transitions in Josephson junctions with antiferromagnetic interlayers, *Phys. Rev. Lett.* **96**, 117005 (2006).
- [29] M. F. Jakobsen, K. B. Naess, P. Dutta, A. Brataas, and A. Qaiumzadeh, Electrical and thermal transport in antiferromagnet-superconductor junctions, *Phys. Rev. B* **102**, 140504(R) (2020).
- [30] M. Hübener, D. Tikhonov, I. A. Garifullin, K. Westerholt, and H. Zabel, The antiferromagnet/superconductor proximity effect in Cr/V/Cr trilayers, *J. Phys.: Condens. Matter* **14**, 8687 (2002).
- [31] C. Bell, E. J. Tarte, G. Burnell, C. W. Leung, D.-J. Kang, and M. G. Blamire, Proximity and Josephson effects in superconductor/antiferromagnetic Nb/ γ -Fe₅₀Mn₅₀ heterostructures, *Phys. Rev. B* **68**, 144517 (2003).
- [32] B. L. Wu, Y. M. Yang, Z. B. Guo, Y. H. Wu, and J. J. Qiu, Suppression of superconductivity in Nb by IrMn in IrMn/Nb bilayers, *Appl. Phys. Lett.* **103**, 152602 (2013).
- [33] R. L. Seeger, G. Forestier, O. Gladii, M. Leiviskä, S. Auffret, I. Joumard, C. Gomez, M. Rubio-Roy, A. I. Buzdin, M. Houzet, and V. Baltz, Penetration depth of Cooper pairs in the IrMn antiferromagnet, *Phys. Rev. B* **104**, 054413 (2021).
- [34] A. Mani, T. G. Kumary, D. Hsu, J. G. Lin, and C.-H. Chern, Modulation of superconductivity by spin canting in a hybrid antiferromagnet/superconductor oxide, *Appl. Phys. Lett.* **94**, 072509 (2009).
- [35] A. Mani, T. G. Kumary, and J. G. Lin, Thickness controlled proximity effects in C-type antiferromagnet/superconductor heterostructure, *Sci. Rep.* **5**, 12780 (2015).
- [36] L. G. Johnsen, S. H. Jacobsen, and J. Linder, Magnetic control of superconducting heterostructures using compensated antiferromagnets, *Phys. Rev. B* **103**, L060505 (2021).
- [37] G. A. Bobkov, I. V. Bobkova, A. M. Bobkov, and A. Kamra, Néel proximity effect at antiferromagnet/superconductor interfaces, *Phys. Rev. B* **106**, 144512 (2022).
- [38] A. F. Volkov, F. S. Bergeret, and K. B. Efetov, Odd triplet superconductivity in superconductor-ferromagnet multilayered structures, *Phys. Rev. Lett.* **90**, 117006 (2003).
- [39] Y. V. Fominov, A. A. Golubov, T. Y. Karminskaya, M. Y. Kupriyanov, R. G. Deminov, and L. R. Tagirov, Superconducting triplet spin valve, *JETP Lett.* **91**, 308 (2010).
- [40] P. V. Leksin, N. N. Garif'yanov, I. A. Garifullin, Y. V. Fominov, J. Schumann, Y. Krupskaya, V. Kataev, O. G. Schmidt, and B. Büchner, Evidence for triplet superconductivity in a superconductor-ferromagnet spin valve, *Phys. Rev. Lett.* **109**, 057005 (2012).
- [41] S. Chourasia, L. J. Kamra, I. V. Bobkova, and A. Kamra, Generation of spin-triplet Cooper pairs via a canted antiferromagnet, *Phys. Rev. B* **108**, 064515 (2023).
- [42] J. Zhu, *Bogoliubov-de Gennes Method and Its Applications*, Lecture Notes in Physics (Springer, Berlin, 2016).
- [43] L. G. Johnsen, N. Banerjee, and J. Linder, Magnetization reorientation due to the superconducting transition in heavy-metal heterostructures, *Phys. Rev. B* **99**, 134516 (2019).
- [44] L. G. Johnsen, K. Svalland, and J. Linder, Controlling the superconducting transition by rotation of an inversion symmetry-breaking axis, *Phys. Rev. Lett.* **125**, 107002 (2020).
- [45] A. H. Morrish, *Canted Antiferromagnetism: Hematite* (World Scientific, Singapore, 1995).

- [46] T. Wimmer, A. Kamra, J. Gückelhorn, M. Opel, S. Geprägs, R. Gross, H. Huebl, and M. Althammer, Observation of antiferromagnetic magnon pseudospin dynamics and the Hanle effect, *Phys. Rev. Lett.* **125**, 247204 (2020).
- [47] A. S. Núñez, R. A. Duine, P. Haney, and A. H. MacDonald, Theory of spin torques and giant magnetoresistance in antiferromagnetic metals, *Phys. Rev. B* **73**, 214426 (2006).
- [48] P. M. Haney, D. Waldron, R. A. Duine, A. S. Núñez, H. Guo, and A. H. MacDonald, *Ab initio* giant magnetoresistance and current-induced torques in Cr/Au/Cr multilayers, *Phys. Rev. B* **75**, 174428 (2007).
- [49] Y. Xu, S. Wang, and K. Xia, Spin-transfer torques in antiferromagnetic metals from first principles, *Phys. Rev. Lett.* **100**, 226602 (2008).
- [50] P. De Gennes, *Superconductivity of Metals and Alloys* (CRC Press, Boca Raton, FL, 2018).